

## RESEARCH ARTICLE

# Region-specific endodermal signals direct neural crest cells to form the three middle ear ossicles

Harinarayana Ankamreddy<sup>1,2</sup>, Hye Hyun Min<sup>1</sup>, Jae Yoon Kim<sup>1,2</sup>, Xiao Yang<sup>4</sup>, Eui-Sic Cho<sup>5</sup>, Un-Kyung Kim<sup>6,7</sup> and Jinwoong Bok<sup>1,2,3,\*</sup>

## ABSTRACT

Defects in the middle ear ossicles – malleus, incus and stapes – can lead to conductive hearing loss. During development, neural crest cells (NCCs) migrate from the dorsal hindbrain to specific locations in pharyngeal arch (PA) 1 and 2, to form the malleus-incus and stapes, respectively. It is unclear how migratory NCCs reach their proper destination in the PA and initiate mesenchymal condensation to form specific ossicles. We show that secreted molecules sonic hedgehog (SHH) and bone morphogenetic protein 4 (BMP4) emanating from the pharyngeal endoderm are important in instructing region-specific NCC condensation to form malleus-incus and stapes, respectively, in mouse. Tissue-specific knockout of *Shh* in the pharyngeal endoderm or *Smo* (a transducer of SHH signaling) in NCCs causes the loss of malleus-incus condensation in PA1 but only affects the maintenance of stapes condensation in PA2. By contrast, knockout of *Bmp4* in the pharyngeal endoderm or *Smad4* (a transducer of TGF $\beta$ /BMP signaling) in the NCCs disrupts NCC migration into the stapes region in PA2, affecting stapes formation. These results indicate that region-specific endodermal signals direct formation of specific middle ear ossicles.

**KEY WORDS:** Middle ear, Ossicles, Conductive hearing loss, Neural crest, Endoderm, Sonic hedgehog, Bone morphogenetic protein 4, Mouse

## INTRODUCTION

The peripheral auditory system in mammals comprises three distinct parts: the outer, middle and inner ear. Sound waves collected by the outer ear are converted into vibrations at the tympanic membrane and these vibrations, amplified by the chain of three ossicles in the middle ear, the malleus, incus and stapes, are relayed to the cochlea of the inner ear (Anthwal and Thompson, 2016). At the cochlea, these mechanical signals are converted by the sensory hair cells into chemical signals, which activate the innervating cochlear nerves to generate electrical impulses that are transmitted to the brain. Each

ossicle has a unique structure and function to efficiently transmit and amplify sound from the environment (Ozeki-Satoh et al., 2016). A break in this transmission, such as ossicular malformations or stapes ankylosis, can result in conductive hearing loss (Quesnel et al., 2015).


Middle ear ossicles are derived from neural crest cells (NCCs; Anthwal and Thompson, 2016; Chapman, 2011). In the craniofacial region, NCCs migrate from the dorsal neural tube and populate the mesenchymal area between the ectodermal and endodermal layers of the pharyngeal arches (PAs; also known as branchial arches). NCCs that originate from the posterior midbrain and the 1st and 2nd rhombomeres of the hindbrain migrate to PA1 and condense to a single cartilage structure that is later separated to form the malleus and incus as well as Meckel's cartilage (Fig. 1H). In contrast, NCCs that originate from the 4th rhombomere migrate to PA2 and give rise to the stapes and hyoid cartilage (Fig. 1H; Bhatt et al., 2013; Minoux and Rijli, 2010). It has been shown that the anterior and posterior identity of the NCCs is pre-determined by their origin in the hindbrain (Minoux and Rijli, 2010). Thus, NCCs that form malleus-incus and stapes are thought to be fated prior to migration into PA1 and PA2, respectively (Bhatt et al., 2013; Minoux and Rijli, 2010).

Signals from the pharyngeal endoderm such as SHH, BMP4 and fibroblast growth factors (FGFs) play important roles in instructing the size, shape and location of NCCs during development of cartilage and bone in the craniofacial region (Abu-Issa et al., 2002; Chapman, 2011; Couly et al., 2002; Jeong et al., 2004; Kanzler et al., 2000; Moore-Scott and Manley, 2005). Some of these molecules have also been implicated in middle ear ossicle development. Notably, disturbance of SHH signaling in NCCs causes developmental defects in nearly all NCC-derived craniofacial cartilage and bone, including middle ear ossicles (Billmyre and Klingensmith, 2015; Jeong et al., 2004). These defects resulted from increased cell death and decreased cell proliferation in the mesenchymal layers of PAs, where NCCs are populated. Inactivation of FGF signaling in mice has also been demonstrated to cause severe craniofacial defects, including loss of middle ear ossicles due to massive cell death in the PAs (Abu-Issa et al., 2002; Trumpp et al., 1999). Although both SHH and FGF signaling have broad effects on PA-derived structures, their specific requirements in ossicle formation are not well defined. It is also unclear how the ossicular NCCs find their proper locations within the two PAs and initiate mesenchymal condensation to form specific ossicles that are in perfect alignment with each other as well as the outer and inner ears.

In this study, we investigated the roles of SHH and BMP4 signaling in middle ear ossicle formation in mouse. We generated endodermal-specific knockouts of *Shh* or *Bmp4* as well as NCC-specific knockouts, which are compromised in their ability to respond to these signaling molecules. Our results show that endodermal SHH signaling is essential for NCCs to initiate mesenchymal condensation to form the malleus and incus in the

<sup>1</sup>Department of Anatomy, Yonsei University College of Medicine, Seoul, South Korea. <sup>2</sup>BK21 PLUS Project for Medical Science, Yonsei University College of Medicine, Seoul, South Korea. <sup>3</sup>Department of Otorhinolaryngology, Yonsei University College of Medicine, Seoul, South Korea. <sup>4</sup>State Key Laboratory of Proteomics, Beijing Proteome Research Center, National Center for Protein Sciences (Beijing), Beijing Institute of Lifeomics, Beijing 102206, China. <sup>5</sup>Cluster for Craniofacial Development and Regeneration Research, Institute of Oral Biosciences, Chonbuk National University School of Dentistry, Jeonju, South Korea. <sup>6</sup>Department of Biology, College of Natural Sciences, Kyungpook National University, Daegu, South Korea. <sup>7</sup>School of Life Sciences, BK21 Plus KNU Creative BioResearch Group, Kyungpook National University, Daegu, South Korea.

\*Author for correspondence (bokj@yuhs.ac)

 X.Y., 0000-0002-0298-9831; J.B., 0000-0003-1958-1872

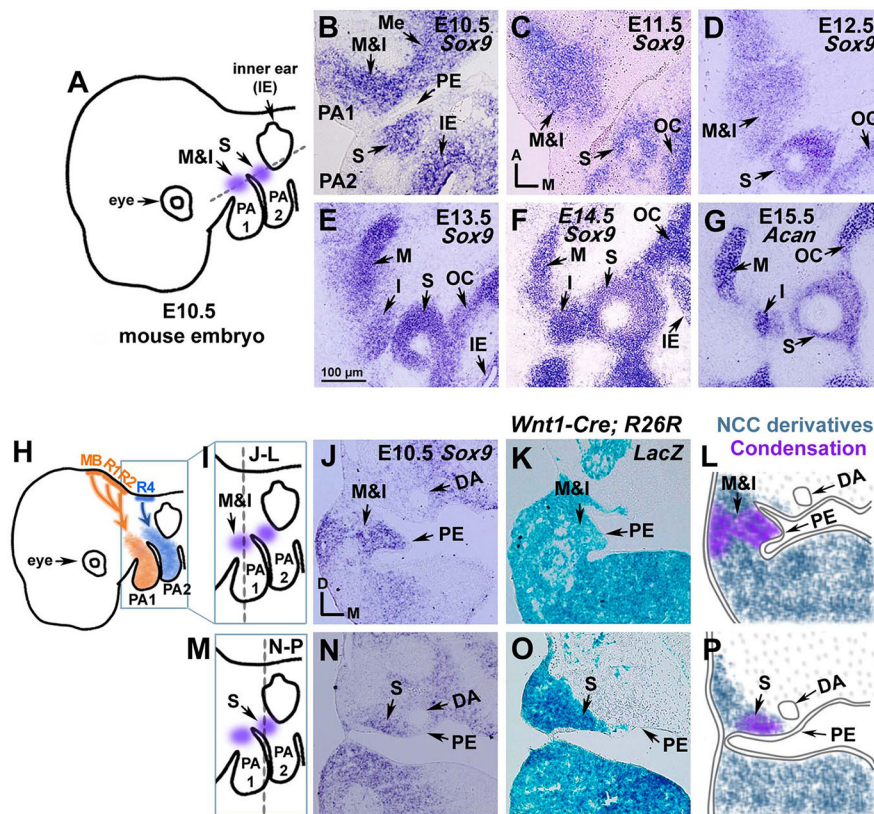


**Fig. 1. Early development of middle ear ossicles in mice.** (A) Schematic of an E10.5 mouse embryo showing the approximate section plane used for B-G (indicated by dashed lines). (B-G) Early development of middle ear ossicles was observed from E10.5 to E15.5 using *Sox9* to identify mesenchymal condensation (B-F) and *Acan* to identify cartilage formation (G). In B-G, anterior is up, medial is right. (H) Diagram indicating that NCCs originating from the posterior midbrain (MB), rhombomere (R)1 and R2 migrate into PA1 (orange arrows and aggregates in PA1), and those originating from R4 migrate into PA2 (blue arrow and aggregates in PA2). (I,M) Schematics of E10.5 mouse embryos showing the section planes (indicated by dashed lines) used for malleus-incus (I) and stapes (M) analysis. (J,N) *Sox9* expression was observed in the malleus-incus (J) and stapes (N) regions. (K,O) Lineage analyses to identify *Wnt1*-expressing NCC derivatives using *Wnt1-Cre; R26R* embryos. (L,P) Diagrams illustrating the spatial relationship between the NCC derivatives (blue) and mesenchymal condensation (purple) in the malleus-incus (L) and stapes (P) regions. DA, dorsal aorta; I, incus; IE, inner ear; M, malleus; Me, Meckel's cartilage; OC, otic capsule; PE, pharyngeal endoderm; S, stapes. In J-N, dorsal is up, medial is right. Scale bar: 100  $\mu$ m.

PA1, whereas endodermal BMP4 signaling is required for stapelial condensation in the PA2.

## RESULTS

### Temporal development of the middle ear ossicles in mice

We analyzed the earliest stage of middle ear development using expression of *Sox9* as an indicator for mesenchymal condensation and aggrecan (*Acan*) as a cartilage marker from embryonic day (E) 10.5 to E15.5 (Fig. 1A-G). In addition, *Hoxa2* was used to demarcate the border between PA1 and PA2 (Minoux and Rijli, 2010), and *Bapx1* (*Nkx3-2*) was used to follow the condensation in PA1 for the malleus-incus and Meckel's cartilage (Tucker et al., 2004). The *Sox9*-positive condensation of NCCs to form the middle ear ossicles is first evident at E10.5 in the mesenchymal regions of PA1 and PA2 (Fig. 1A,B; Fig. S1A-C). The border between PA1 and PA2 was evident by the restricted expression of *Hoxa2* in the mesenchyme of PA2 from E10.5 to E12.5 (Fig. S1B,F,I). The single condensation in PA1 gradually separates to form the malleus and incus by E13.5 (Fig. 1B-E; Fig. S1). *Bapx1* was expressed in the mesenchyme medial to the malleus-incus condensation at E11.5 and later in the mesenchyme surrounding the malleus at E13.5 (Fig. S1G,J,M). The condensation in PA2 for the stapes starts to acquire its unique 'stirrup' shape at E11.5 (Fig. 1C; Fig. S1E) and is connected to the otic capsule of the inner ear by E13.5 (Fig. 1E). *Hoxa2* expression in PA2 partially overlapped with stapes condensation at E10.5 and E11.5 and was downregulated in the stapes at E12.5 (Fig. S1B,F,I,L). The *Sox9*-positive ossicular condensations become *Acan* positive by E15.5 (Fig. 1G).

To confirm that these ossicle-related condensations observed in PA1 and PA2 are derived from NCCs, we compared the *Sox9* expression domains with NCC lineage tracing by crossing *Wnt1-Cre* mice with a Cre reporter, *Rosa26-lacZ* (*R26R*) mice (Chai et al., 2000) (Fig. 1I-P). In coronal sections (Fig. 1I,M), *Sox9* expression

in the malleus-incus condensation was observed in the mesenchyme lateral to the pharyngeal endoderm in the PA1 region (Fig. 1J), whereas *Sox9* expression for stapelial condensation was observed in the mesenchyme dorsal to the pharyngeal endoderm in the PA2 region (Fig. 1N). The *lacZ*-positive NCC lineage cells (identified by X-gal staining) were populated broadly in the mesenchymal regions of PA1 and PA2, which encompassed the *Sox9*-positive condensation areas for both the malleus-incus and stapes (Fig. 1J-L, N-P). Together, these results show that the identified condensations of middle ear ossicles at E10.5 in PA1 and PA2 are part of the NCC lineage.

### SHH signaling is required for initial condensation of the malleus-incus but not of the stapes

SHH signaling has been shown to play important roles in normal development of craniofacial structures, including the middle ear ossicles, by promoting proliferation and survival of NCCs in the mesenchymal layers of PAs (Jeong et al., 2004); however, it remains unclear whether SHH signaling contributes to early stages of middle ear development, such as migration and condensation of NCCs in the prospective ossicular regions. We thus examined the spatial relationship between the initial condensation of middle ear ossicles and SHH signaling at E10.5 (Fig. 2). In a cross-section of the PA1 region (Fig. 2K), *Shh* is broadly expressed in the pharyngeal endoderm (Fig. 2A), and *Ptch1*, a readout of SHH signaling, is expressed in the surrounding mesenchyme in a graded pattern (Fig. 2B). The malleus-incus condensation overlapped with the graded *Ptch1* expression domain (Fig. 2C). In contrast, *Shh* expression was specifically absent in the pharyngeal endoderm just beneath the stapes condensation (Fig. 2L, red bracket). *Ptch1* expression was also much weaker in the stapes condensation compared with the mesenchyme surrounding the endoderm (Fig. 2M,N, red bracket). These results indicate that endodermal

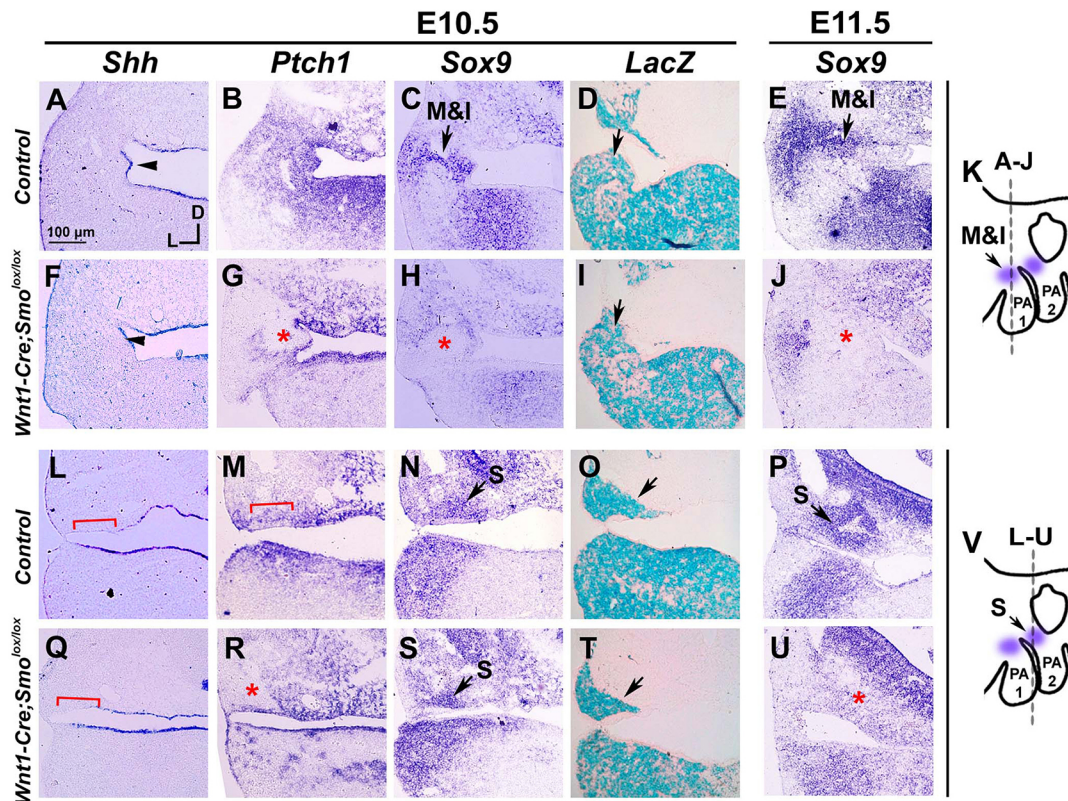


**Fig. 2. Inactivation of SHH signaling in NCCs results in loss of initial condensation of malleus-incus but not of stapes.** (A–J) Expression of *Shh* (A,F), *Ptch1* (B,G), *Sox9* (C,E,H,J) in the malleus-incus region was compared between control (A–E) and *Wnt1-Cre; Smo<sup>lox/lox</sup>* (F–J) embryos at E10.5 (A–D,F–I) and E11.5 (E,J). Expression of *Shh* in the endoderm was not changed in *Wnt1-Cre; Smo<sup>lox/lox</sup>* embryos (A,F; arrowheads). Expression of *Ptch1* (G; red asterisk) and *Sox9* (H,J; red asterisks) was greatly reduced in *Wnt1-Cre; Smo<sup>lox/lox</sup>* embryos. (L–U) Expression of *Shh* (L,Q), *Ptch1* (M,R), *Sox9* (N,P,S,U) in the stapes region was compared between control (L–P) and *Wnt1-Cre; Smo<sup>lox/lox</sup>* (Q–U) embryos at E10.5 (L–O,Q–T) and E11.5 (P,U). Red square brackets in L and Q indicate no *Shh* expression in the pharyngeal endoderm. Weak *Ptch1* expression shown in the stapes region in control embryos (M, red bracket) was greatly reduced in *Wnt1-Cre; Smo<sup>lox/lox</sup>* embryos (R; red asterisk). In contrast, *Sox9* expression was present in the stapes region at E10.5 (S; arrow) but not at E11.5 (U; red asterisk) in *Wnt1-Cre; Smo<sup>lox/lox</sup>* embryos. (D,I,O,T) Lineage analysis using X-gal staining to detect *lacZ* expression in malleus-incus (D,I) and stapes (O,T) regions of control (D,O) and *Wnt1-Cre; Smo<sup>lox/lox</sup>* (I,T) embryos. *lacZ*-positive NCC derivatives were present in both malleus-incus and stapes regions (D,I,O,T; arrows). (K,V) Schematics of E10.5 mouse embryos showing the section planes (indicated by dashed lines) used for malleus-incus (K) and stapes (V) analysis. I, incus; M, malleus; S, stapes. In all images, dorsal is up and lateral is left. Scale bar: 100  $\mu$ m.

SHH signaling is much stronger neighboring the condensation for malleus-incus than for stapes, raising the possibility that SHH signaling plays differential roles in the condensation of the middle ear ossicles.

We tested this hypothesis by inactivating the ability of NCCs to respond to SHH by deleting the transducer of SHH signaling, *Smo*, in NCCs using *Wnt1-Cre*. In *Wnt1-Cre; Smo<sup>lox/lox</sup>* mutants, *Ptch1* expression was greatly reduced in the mesenchyme where NCCs normally populate both PA1 and PA2 at E10.5 (Fig. 2G,R, red asterisks), whereas *Shh* expression in the pharyngeal endoderm was unaffected (Fig. 2F,Q), suggesting that SHH signaling is specifically inactivated in NCC derivatives in *Wnt1-Cre; Smo<sup>lox/lox</sup>* mutant embryos. Interestingly, *Sox9* expression in PA1 was selectively abolished in the area where malleus-incus condensation normally occurs (Fig. 2H, red asterisk). In contrast, *Sox9* expression associated with stapes condensation, though reduced, remained in PA2 at E10.5 (Fig. 2S, arrow). These results suggest that NCCs require SHH signaling to initiate mesenchymal condensation for the malleus-incus but not for the stapes.

The lack of malleus-incus condensation in *Wnt1-Cre; Smo<sup>lox/lox</sup>* mutant embryos may be due to either a failure of NCC migration to the malleus-incus region or a failure of NCC condensation or survival after migration. It has been reported that SHH signaling

is not essential for NCC migration but is essential for NCC condensation and survival (Billmyre and Klingensmith, 2015; Brito et al., 2006; Jeong et al., 2004). To follow the lineage of NCC derivatives, we genetically labeled NCC derivatives by crossing *Wnt1-Cre; Smo<sup>lox/lox</sup>* mice with R26R-*lacZ* mice. Interestingly, *lacZ*-positive cells were present in the prospective malleus-incus region even though no clear malleus-incus condensation was detected (Fig. 2D,I). These results suggest that NCCs migrate to the malleus-incus region but fail to initiate condensation in the absence of SHH signaling.

### SHH signaling is required for survival of NCCs during middle ear development

When *Sox9* expression was examined in *Wnt1-Cre; Smo<sup>lox/lox</sup>* embryos at E11.5, the malleus-incus condensation remained absent (Fig. 2E,J, red asterisk), suggesting that the lack of malleus-incus condensation is not due to a developmental delay. Interestingly, the stapes condensation, which was present at E10.5 (Fig. 2N,S), had disappeared by E11.5 (Fig. 2P,U, red asterisk). Consistent with this, no middle ear cartilages were observed in *Wnt1-Cre; Smo<sup>lox/lox</sup>* embryos at E15.5 (Fig. 3B, red asterisks). These results indicate that SHH signaling, which is dispensable for the initial condensation of the stapes, is required for the maintenance of this condensation.

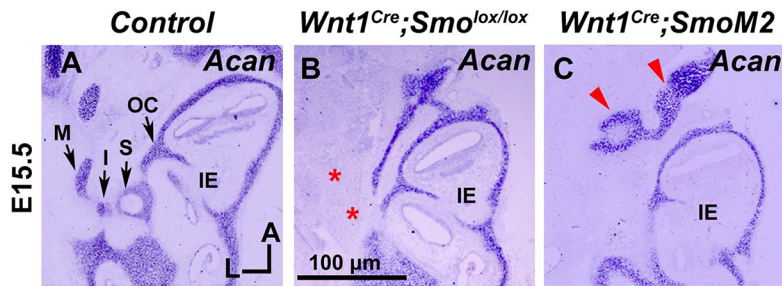


**Fig. 3. Middle ear phenotypes in mutants with loss or gain of SHH function in NCCs.** (A-C) *Acan* expression in the middle ear cartilages was compared between controls (A), *Wnt1-Cre; Smo<sup>lox/lox</sup>* (B) and *Wnt1-Cre; SmoM2* (C) mutant embryos at E15.5. All middle ear ossicles were lost in *Wnt1-Cre; Smo<sup>lox/lox</sup>* embryos (B; red asterisks). All middle ear ossicles were fused together and dislocated from their normal positions in *Wnt1-Cre; SmoM2* embryos (C; arrowheads). I, incus; IE, inner ear; M, malleus; OC, otic capsule; S, stapes. In all images, anterior is up, lateral is left. Scale bar: 100  $\mu$ m.

Because SHH signaling is important for NCC proliferation and survival during craniofacial development (Ahlgren and Bronner-Fraser, 1999; Brito et al., 2006; Jeong et al., 2004), we determined whether the loss of ossicular condensation in *Wnt1-Cre; Smo<sup>lox/lox</sup>* embryos was due to abnormal NCC proliferation or survival. Cell proliferation was analyzed by counting the number of cells that had incorporated 5-ethynyl-2'-deoxyuridine (EdU) in the condensation areas (Fig. 4A-B',F-G'). No significant difference in the number of EdU-positive cells between control and *Wnt1-Cre; Smo<sup>lox/lox</sup>* embryos was detected (Fig. 4K). In contrast, the number of terminal deoxynucleotidyl transferase dUTP nick end labeling (TUNEL)-positive cells was significantly increased in both the malleus-incus and stapedial condensation areas in *Wnt1-Cre; Smo<sup>lox/lox</sup>* embryos compared with control embryos (Fig. 4C-D',H-I',L). These results indicate that although SHH signaling plays differential roles in the initial condensation of the malleus-incus in PA1 and the stapes in PA2, this signaling pathway is essential for NCC survival in both PAs regardless of condensation status.

### SHH signaling essential for ossicular condensation emanates from the pharyngeal endoderm

Next, we investigated whether SHH from the pharyngeal endoderm is important for condensation of the malleus-incus and maintenance of the stapes. To delete *Shh* in the endodermal epithelium specifically,

*Shh<sup>lox/lox</sup>* mice were crossed with *Foxg1<sup>Cre</sup>* mice, which have been shown to induce Cre-mediated recombination in the foregut epithelium (Hébert and McConnell, 2000). In *Foxg1<sup>Cre</sup>; Shh<sup>lox/lox</sup>* embryos, endodermal *Shh* as well as mesenchymal *Ptch1* expression were completely abolished in both PA1 and PA2 (Fig. 5F,G,Q,R, red asterisks). Consistent with inactivation of SHH signaling in the NCCs (Fig. 2), *Sox9* expression was strongly downregulated in the malleus-incus condensation area in PA1 (Fig. 5C,H, red asterisk), whereas *Sox9* expression was present, although reduced, in the stapedial condensation in PA2 (Fig. 5N,S, arrows). Examination of *Tfap2a* expression to identify migrating NCCs indicated that this gene was not expressed in the prospective malleus and incus region in PA1 but was expressed in the stapes region in PA2 (Fig. 5D,I,O,T). Consistent with previous results (Fig. 2P,U), condensations for both malleus-incus and stapes were not present at E11.5 in these animals (Fig. 5P, U, red asterisk). It should be noted that the Cre activity of *Foxg1<sup>Cre</sup>* is also detectable in areas of pharyngeal ectoderm and mesoderm (Tavares et al., 2012). In addition, we noticed that PA development is severely disrupted in *Foxg1<sup>Cre</sup>; Shh<sup>lox/lox</sup>* embryos. Thus, the middle ear phenotypes of *Foxg1<sup>Cre</sup>; Shh<sup>lox/lox</sup>* embryos may be confounded by malformed PA structures as well as contributions from other sources. Nevertheless, our results strongly suggest that SHH emanating from the pharyngeal endoderm plays an essential role in the condensation and maintenance of the ossicles.

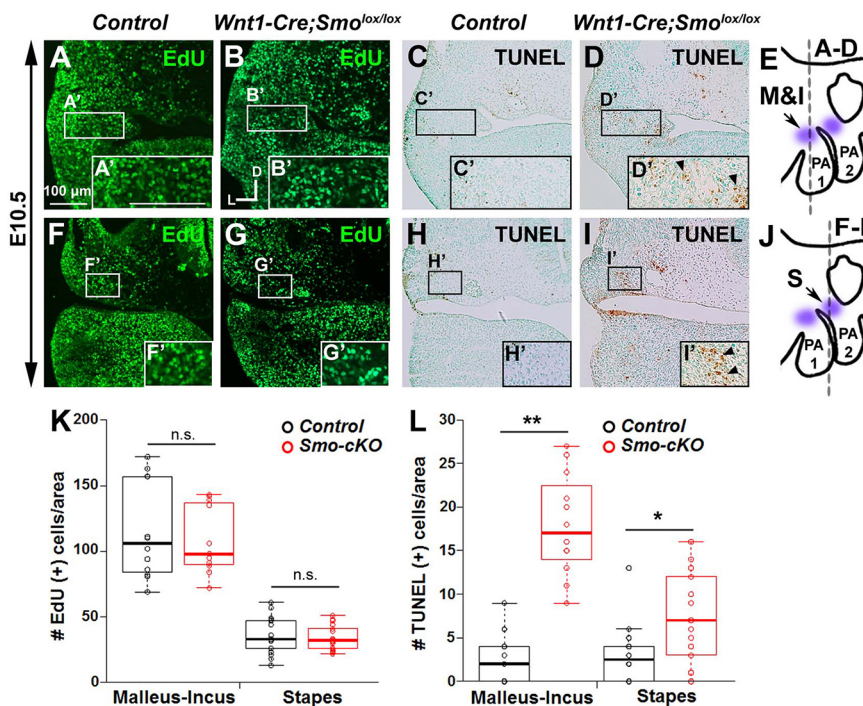


**Fig. 4. Inactivation of SHH signaling in NCCs causes cell death in middle ear condensation regions.**

(A,B,F,G) Proliferating cells were visualized by EdU staining in the malleus-incus (A,B) and stapes (F,G) regions in control (A,F) and *Wnt1-Cre; Smo<sup>lox/lox</sup>* (B,G) embryos. (C-D',H-I') Apoptotic cells were visualized by TUNEL staining in the malleus-incus (C,D) and stapes (H,I) regions in control (C,H) and *Wnt1-Cre; Smo<sup>lox/lox</sup>* (D,I) embryos. TUNEL-positive cells were increased in *Wnt1-Cre; Smo<sup>lox/lox</sup>* embryos (D,I; arrowheads). Insets show magnifications of the boxed areas, as indicated. (E,J) Schematics of E10.5 mouse embryos showing the section planes (indicated by dashed lines) used for malleus-incus (E) and stapes (J). (K,L) Quantification of EdU-positive (K) and TUNEL-positive (L) cells within the boxes (shown in A'-D' and F'-I') of condensation regions in control and *Wnt1-Cre; Smo<sup>lox/lox</sup>* embryos. Three samples per each genotype were analyzed. Data are displayed as box plots. Individual dots represent individual data values, the boxes represent a range of 25-75%, the horizontal lines in the boxes represent the median, the whiskers represent the maximum and minimum values, and the points outside the whiskers represent outliers. \* $P < 0.05$ , \*\* $P < 0.01$ , as determined by Student's *t*-tests. n.s., not significant ( $P > 0.05$ ). Scale bar: 100  $\mu$ m.

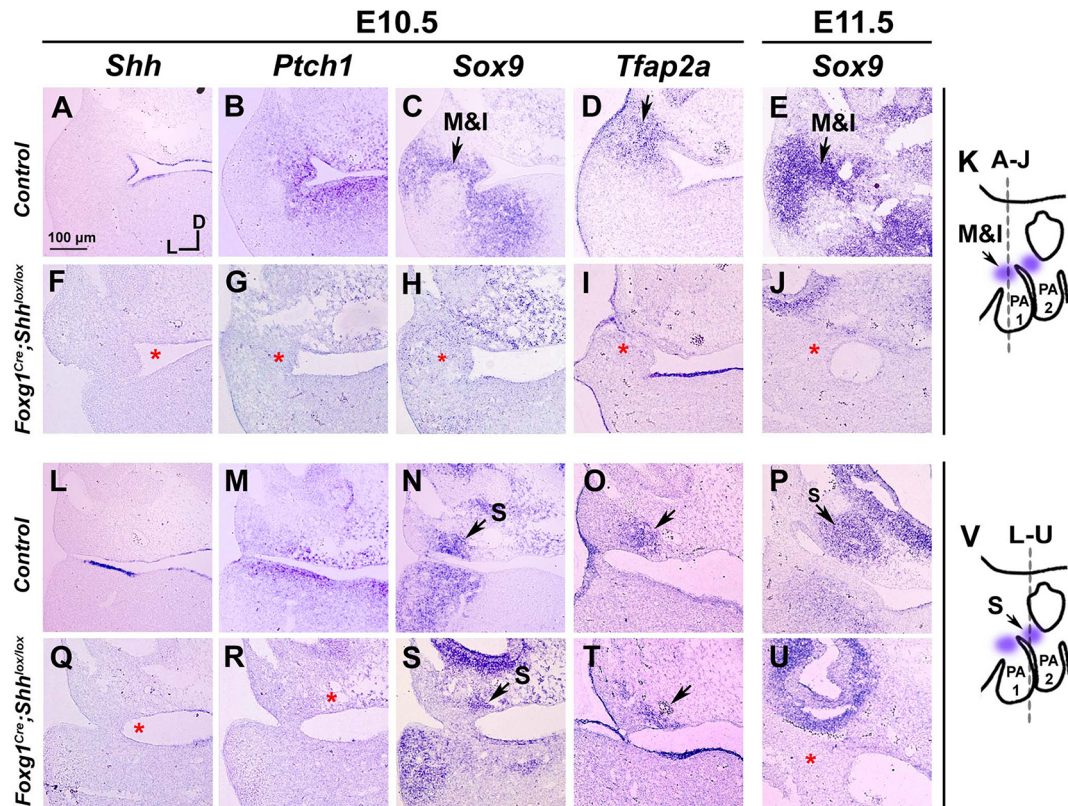


**Fig. 5. Deletion of *Shh* in the pharyngeal endoderm results in loss of initial condensation of malleus-incus but not of stapes.** (A–J) Expression of *Shh* (A,F), *Ptch1* (B,G), *Sox9* (C,E,H,J) and *Tfap2a* (D,I) in the malleus-incus region was compared between control (A–E) and *Foxg1<sup>Cre</sup>; Shh<sup>lox/lox</sup>* (F–J) embryos at E10.5 (A–D,F–I) and E11.5 (E,J). Expression of *Shh*, *Ptch1*, *Sox9* and *Tfap2a* was lost in *Foxg1<sup>Cre</sup>; Shh<sup>lox/lox</sup>* embryos (F–J; red asterisks). (L–U) Expression of *Shh* (L,Q), *Ptch1* (M,R), *Sox9* (N,P,S,U) and *Tfap2a* (O,T) in the stapes region was compared between control (L–P) and *Foxg1<sup>Cre</sup>; Shh<sup>lox/lox</sup>* (Q–U) embryos at E10.5 (L–O,Q–T) and E11.5 (P,U). Expression of *Shh* and *Ptch1* was lost (Q,R; red asterisks), whereas expressions of *Sox9* and *Tfap2a* were present although reduced (S,T; arrows) in *Foxg1<sup>Cre</sup>; Shh<sup>lox/lox</sup>* embryos. *Sox9* expression in the stapes region was lost at E11.5 (U; red asterisk). (K,V) Schematics of E10.5 mouse embryos showing section planes (indicated by dashed lines) used for malleus-incus (K) and stapes (V) analysis. I, incus; M, malleus; S, stapes. In all images, dorsal is up and lateral is left. Scale bar: 100  $\mu$ m.

### Constitutive activation of SHH signaling in the NCCs impairs normal middle ear development

Forced expression of *Shh* in the chondrocytes disrupts normal limb cartilage development by affecting cell proliferation and apoptosis, resulting in impaired joint formation (Tavella et al., 2006, 2004). We thus investigated whether constitutive activation of SHH signaling in NCCs affects middle ear development. To activate SHH signaling constitutively in NCCs, we used *Wnt1-Cre; SmoM2* mutant embryos, in which a constitutively active form of *Smo* was expressed in NCC derivatives (Jeong et al., 2004). In *Wnt1-Cre; SmoM2* embryos, *Ptch1* expression was expanded in the entire mesenchymal region where NCCs normally reside (Fig. S2D,K, arrowheads). *Sox9* expression in the ossicular condensation was also increased in *Wnt1-Cre; SmoM2* embryos compared with control embryos at E10.5 (Fig. S2E,L); however, the number of EdU-positive cells in the middle ear condensation regions were not significantly different between control and *Wnt1-Cre; SmoM2* embryos (Fig. S2C,F,J,M,O). This finding suggests that the enlarged condensation is not due to increased proliferation but rather an upregulation of *Sox9* expression (Tavella et al., 2004). In E15.5 *Wnt1-Cre; SmoM2* embryos, the middle ear cartilages were fused together and displaced from the prospective oval window of the otic capsule (Fig. 3C, arrowheads). These results suggest that tight regulation of SHH signaling in the NCCs is important for normal development and localization of middle ear ossicles.

### BMP signaling is required for NCC migration and condensation for the stapes

The presence of the stapelial condensation in the absence of SHH signaling suggests that other signaling pathways are at play in the PA2 region for mediating NCC condensation. In addition to *Shh*, it has been shown that *Fgf8* and *Bmp4* are expressed in the pharyngeal endoderm and play essential roles in patterning the PA-derived structures (Moore-Scott and Manley, 2005). However, in *Fgf8*-null embryos, the stapes was found to be normal or only slightly smaller than in control embryos (Abu-Issa et al., 2002), excluding a requirement for FGF8 in the initial condensation of stapes. In contrast, BMP signaling is important for chondrogenesis and functions by regulating the induction and maintenance of *Sox9* expression *in vitro* and *in vivo* (Bandyopadhyay et al., 2006; Kumar et al., 2012; Semba et al., 2000). Interestingly, we found that *Bmp4* was specifically expressed in the endodermal epithelium just beneath the stapes condensation in PA2 (Fig. 6E,F, bracket) but not adjacent to the malleus-incus or hyoid condensation (Fig. 6A,B, I,J). In addition, *Shh*, which is broadly expressed in the entire pharyngeal endoderm, was specifically absent in the *Bmp4* expression domain (Fig. 6C,F,G,K, brackets).

These spatial relationships suggest a possible role for endodermal BMP4 signaling in NCC migration and condensation for stapes development. We tested this possibility by inactivating the ability of NCCs to respond to TGF $\beta$ /BMP signaling by deleting *Smad4* in NCCs using *Wnt1-Cre* (Fig. 7). In E10.5 *Wnt1-Cre; Smad4<sup>lox/lox</sup>*

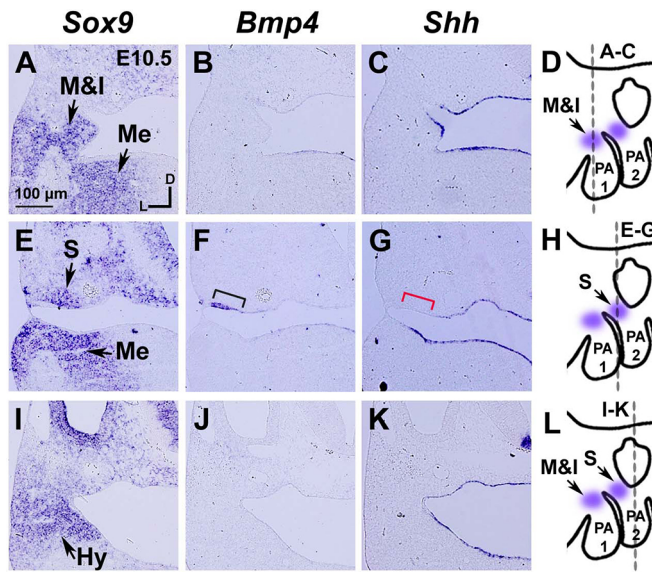


**Fig. 6. *Bmp4* expression in the endoderm is closely associated with stapes condensation.** (A-L) Expression of *Sox9*, *Bmp4* and *Shh* was compared in the malleus-incus (A-C), stapes (E-G), hyoid (I-K) condensation regions in E10.5 control embryos. (D,H,L) Schematics of E10.5 mouse embryos showing the section planes (indicated by dashed lines) used for malleus-incus (D), stapes (H) and hyoid (L) region analysis. Black arrows indicate *Sox9* expression in condensation regions for malleus and incus (M&I), Meckel's cartilage (Me), stapes (S) and hyoid cartilage (Hy). *Bmp4* was specifically expressed (F; black square bracket) and *Shh* was specifically absent (G; red square bracket) in the pharyngeal endoderm just beneath the stapes condensation. In all images, dorsal is up and lateral is left. Scale bar: 100  $\mu$ m.

embryos, *Sox9* expression was completely downregulated in the stapelial condensation area (Fig. 7M,R, red asterisk), whereas expression in the malleus-incus condensation area was unaffected (Fig. 7B,G, arrows). These results indicate that TGF $\beta$ /BMP signaling is selectively required for NCCs to initiate the mesenchymal condensation for the stapes.

Analysis of cell proliferation and cell death demonstrated that the numbers of EdU- or TUNEL-positive cells in the condensation regions of the malleus-incus (Fig. 7C,D,H,I) and the stapes (Fig. 7N,O,S,T) were not significantly different between control and *Wnt1-Cre; Smad4<sup>lox/lox</sup>* embryos (Fig. 7W,X). Thus, the failure of stapelial condensation of NCCs in the absence of TGF $\beta$ /BMP signaling is unlikely to be due to abnormal cell proliferation or cell death.

As TGF $\beta$ /BMP signaling has been shown to be important for NCC formation and migration (Kanzler et al., 2000), it is possible that the loss of stapes condensation in *Wnt1-Cre; Smad4<sup>lox/lox</sup>* embryos is due to a failure of NCC migration into the stapes region. To test this idea, we first examined normal NCC migration patterns into the prospective ossicular condensation regions from E9.5 to E10.5 (Fig. 8). In PA1, *lacZ*-positive NCC derivatives were present in the prospective malleus-incus region from E9.5 (Fig. 8D,H,L, arrows); however, condensation for the malleus-incus was not evident until E10.5 (Fig. 8A,E,I, arrow). In PA2, *lacZ*-positive NCC derivatives were not detected at E9.5 (Fig. 8Q, asterisk), began to localize in the lateral mesenchyme at E10.0 (Fig. 8U, arrowheads), and expanded medially to the stapes region at E10.5 (Fig. 8Y, arrow) concurrent with initiation of *Bmp4* expression in the endoderm (Fig. 8O,S,W, bracket). Interestingly, in E10.5 *Wnt1-Cre; Smad4<sup>lox/lox</sup>* embryos, *lacZ*-positive NCC

derivatives were restricted in the lateral mesenchyme of the PA2 but not detected in the region where NCCs normally condense to form the stapes (Fig. 7P,U, arrowheads and red asterisk). These results suggest that NCCs fail to migrate to the location where the stapes condensation normally occurs when the TGF $\beta$ /BMP signaling pathway is disrupted.

### BMP signaling essential for NCC migration and stapes condensation emanates from the pharyngeal endoderm

To test whether *Bmp4* expressed in the endoderm is the ligand specifically required for stapes condensation, we deleted *Bmp4* in the endodermal epithelium using *Foxg1<sup>Cre</sup>; Bmp4<sup>lox/Tm1</sup>* mice (Fig. 9K, red bracket). In these embryos, *Sox9* expression in the prospective stapes condensation was lost (Fig. 9I,L, red asterisk), whereas this expression in the malleus-incus condensation was unaffected (Fig. 9B,E, arrow). Consistent with this, *Tfap2a* expression in the migrating NCCs was absent in the stapes condensation area in *Foxg1<sup>Cre</sup>; Bmp4<sup>lox/Tm1</sup>* embryos (Fig. 9J,M, red asterisk). These results demonstrate that endodermal *Bmp4* is specifically required for NCC migration and initial condensation for the stapes but not for the malleus and incus.

We next examined whether the loss of stapes condensation in the absence of TGF $\beta$ /BMP signaling leads to a specific loss of stapes in later development. Previous studies demonstrated that *Foxg1<sup>Cre</sup>; Bmp4<sup>lox/Tm1</sup>* and *Wnt1-Cre; Smad4<sup>lox/lox</sup>* mutants exhibit early embryonic lethality at E13.5 and E12.5, respectively (Chang et al., 2008; Ko et al., 2007). Thus, we examined the middle ear phenotypes at the latest stage that we could harvest the mutant embryos. In *Foxg1<sup>Cre</sup>; Bmp4<sup>lox/Tm1</sup>* embryos, the stapes was specifically absent, whereas development of the malleus and incus appeared normal at E12.5 and E13.5 (Fig. 10G,H,J,K, red asterisks), confirming the specific requirement of endodermal *Bmp4* in stapes development. Similarly, a specific loss of the stapes was observed in *Wnt1-Cre; Smad4<sup>lox/lox</sup>* embryos at E12.5 (Fig. 10G,I, red asterisk). We also noticed, however, that the malleus-incus condensation was much reduced compared with that in control embryos (Fig. 10I, arrow). This result is consistent with a report that *Smad4*-mediated TGF $\beta$ /BMP signaling plays an important role in developmental progression of NCCs during craniofacial development (Ko et al., 2007).

## DISCUSSION

In this study, we investigated how migratory NCCs find their destinations and develop into specific middle ear ossicles. Our results suggest that pharyngeal endoderm provides region-specific signaling molecules to initiate NCC condensation in PA1 or guide NCCs to specific locations within PA2 to differentiate into the three ossicles.

### Region-specific requirements of SHH in middle ear development

The loss of SHH function by either making NCCs unable to mediate SHH signaling (*Wnt1-Cre; Smo<sup>lox/lox</sup>*) or abolishing the expression of *Shh* in the endoderm (*Foxg1<sup>Cre</sup>; Shh<sup>lox/lox</sup>*) resulted in similar phenotypes: failure of initial condensation of the malleus-incus but not of stapes (Fig. 11C,D). Notably, although *Shh* is broadly expressed in the endoderm and specifies malleus-incus condensation, *Shh* expression is specifically absent from the region of the endoderm closely associated with stapelial condensation (Fig. 2 and Fig. 11B). These results suggest that SHH signaling emanating from the endoderm is specifically required for the condensation of NCCs for malleus-incus generation in PA1 but not for the stapes in PA2. However, all

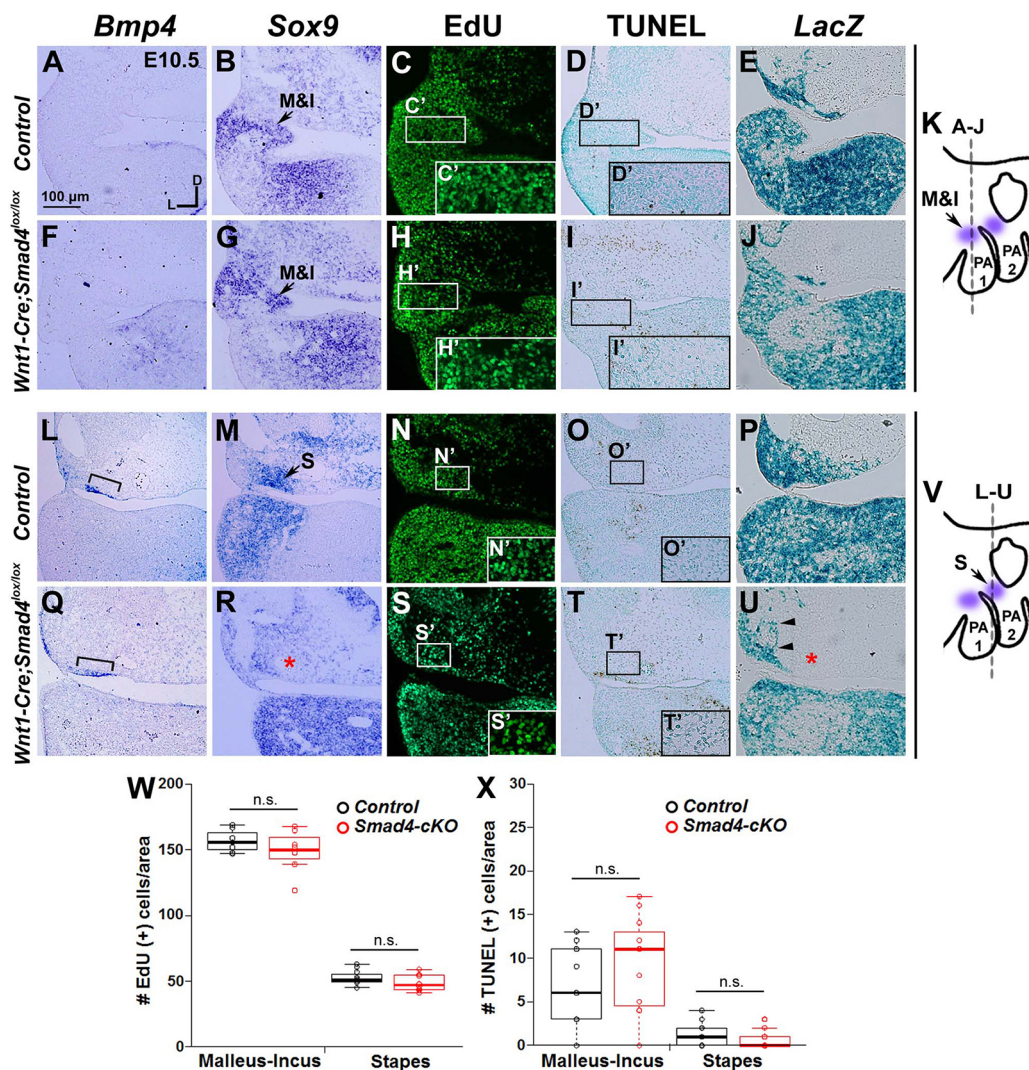


**Fig. 7. Inactivation of TGF $\beta$ /BMP signaling in the NCCs results in loss of initial condensation of stapes but not of malleus-incus.** (A,B,F,G,L,M,Q,R) Expression of *Bmp4* (A,F,L,Q) and *Sox9* (B,G,M,R) was compared in the malleus-incus (A,B,F,G) and stapes (L,M,Q,R) regions of control (A,B,L,M) and *Wnt1-Cre; Smad4<sup>lox/lox</sup>* (F,G,Q,R) embryos. *Sox9* expression in the stapes region was lost in *Wnt1-Cre; Smad4<sup>lox/lox</sup>* embryo (R; red asterisk). (C,H,N,S) Proliferating cells were visualized by EdU staining in the malleus-incus (C,H) and stapes (N,S) regions in control (C,N) and *Wnt1-Cre; Smad4<sup>lox/lox</sup>* (H,S) embryos. (D,I,O,T) Apoptotic cells were visualized by TUNEL staining in the malleus-incus (D,I) and stapes (O,T) regions in control (D,O) and *Wnt1-Cre; Smad4<sup>lox/lox</sup>* (I,T) embryos. (W,X) Quantification of EdU-positive (W) and TUNEL-positive (X) cells within the boxes (shown in the insets C', H', N' and S' for EdU staining and the insets D', I', O' and T' for TUNEL staining) of condensation regions in control and *Wnt1-Cre; Smad4<sup>lox/lox</sup>* embryos. Three samples of each genotype were analyzed. Data are displayed as box plots. Individual dots represent individual data values, the boxes represent a range of 25-75%, the horizontal lines in the boxes represent the median, the whiskers represent the maximum and minimum values, and the points outside the whiskers represent outliers. n.s., not significant ( $P > 0.05$ , as determined by Student's *t*-test). (E,J,P,U) Lineage analysis using *lacZ* detection in malleus-incus (E,J) and stapes (P,U) regions of control (E,P) and *Wnt1-Cre; Smad4<sup>lox/lox</sup>* (J,U) embryos. *lacZ*-positive NCC derivatives were absent in the stapes region (U; red asterisk). (K,V) Schematics of E10.5 mouse embryos showing the section planes (indicated by dashed lines) used for malleus-incus (K) and stapes (V) analysis. I, incus; M, malleus; S, stapes. In all images, dorsal is up and lateral is left. Scale bar: 100  $\mu$ m.

three ossicles were eventually lost in the absence of SHH signaling (Figs 2, 3 and 5) (Billmyre and Klingensmith, 2015; Jeong et al., 2004), indicating that, although the requirements for SHH in condensation differs for each ossicle, the SHH requirement for survival is common for all ossicles.

Currently, how endodermal SHH signaling directs NCCs to initiate condensation in the prospective malleus-incus region remains unknown. In our SHH gain-of-function model (*Wnt1-Cre; SmoM2*), SHH signaling was activated in all *Wnt1*-positive NCC derivatives, resulting in expansion of the *Ptch1* expression domain to mesenchymal areas at a distance from the *Shh*-expressing endoderm (Fig. S2). The *Sox9* expression domain delineating

malleus-incus condensation, however, was only slightly expanded, and this expanded region was restricted to areas around the original condensation domains (Fig. S2). Thus, activation of SHH signaling alone is not sufficient to promote mesenchymal condensation in the migratory NCCs. In addition, *Shh* is expressed broadly throughout the endodermal epithelium of PAs, suggesting that endodermal SHH signaling may not be specific enough to recruit NCCs to the proper location and promote mesenchymal condensation. One such factor could be FGF8, as *Fgf8* is expressed in the ectoderm of PA1 and in the endoderm of PA2, PA3 and PA4 (Abu-Issa et al., 2002;

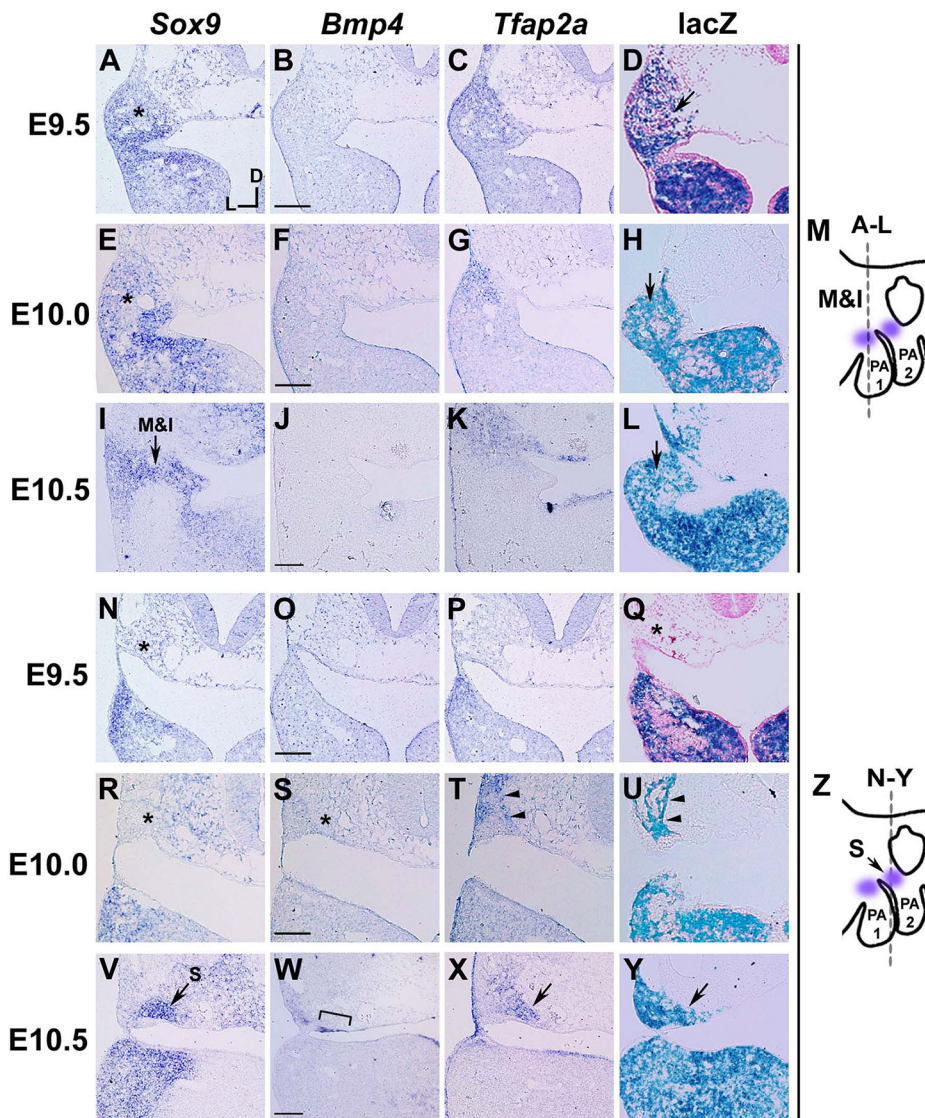


**Fig. 8. Time course of NCC migration into the prospective ossicular condensation regions from E9.5 to E10.5.** Expression of *Sox9* (A,E,I,N,R,V), *Bmp4* (B,F,J,O,S,W), and *Tfap2a* (C,G,K,P,T,X), as well as *lacZ*-positive NCC derivatives (D,H,L,Q,U,Y) were analyzed in the prospective malleus-incus condensation in PA1 (A-L) and in the prospective stapes condensation in PA2 (N-Y) at E9.5 (A-D,N-Q), E10.0 (E-H,R-U) and E10.5 (I-L,V-Y). (M,Z) Schematics of the section planes (indicated by dashed lines) used for malleus-incus (M) and stapes (Z) analysis. (A-D,N-Q) At E9.5, *lacZ*-positive-NCC derivatives were populated in the prospective malleus-incus region (D; arrow), yet there was no clear condensation for the malleus-incus (A; asterisk). In the prospective stapes region, neither *lacZ*-positive NCC derivatives (Q; asterisk) nor condensation (N; asterisk) was observed. (E-H,R-U) At E10.0, *lacZ*-positive NCC derivatives were present in the malleus-incus region (H; arrow), yet no clear condensation for the malleus-incus was observed in PA1 (E; asterisk). In PA2, *Tfap1a* expression and *lacZ*-positive NCC derivatives were detected in the lateral mesenchyme (T,U; arrowheads); yet, there was no indication of the stapes condensation (R; asterisk) or *Bmp4* expression in the endoderm (S; asterisk). (I-L,V-Y) At E10.5, condensations for the malleus-incus in PA1 (I) and the stapes in PA2 (V) were clearly demarcated. *Bmp4* began to be expressed in the endoderm beneath the stapes condensation region (W; bracket). *lacZ*-positive cells were expanded medially into the stapes condensation region (Y; arrow). In addition, *Tfap2* expression was detected in the stapes condensation (X; arrow). I, incus; M, malleus; S, stapes. In all images, dorsal is up and lateral is left. Scale bar: 100  $\mu$ m.

Moore-Scott and Manley, 2005; Trumpp et al., 1999). However, the expression domain of *Fgf8* in the ectoderm of PA1 is not in close proximity to where the malleus-incus develops (data not shown). Therefore, it is not apparent how FGF8 signaling could play a role in directing NCC migration to the malleus-incus region. Nevertheless, mice lacking *Fgf8* also show increased apoptotic cell death in PA1, resulting in the loss of PA1-derived craniofacial structures, including the malleus and incus (Abu-Issa et al., 2002; Moore-Scott and Manley, 2005; Trumpp et al., 1999). The similarity of cell death in the prospective malleus-incus area in both *Fgf8* and *Shh* mutants suggests that ectodermal FGF8 and endodermal SHH are both survival factors for NCCs but whether they function together to specify NCC migration to form malleus and incus remains to be determined.

#### Specific requirement of endodermal BMP4 for stapes condensation

In contrast to the broad expression of *Shh*, *Bmp4* was specifically expressed in the endodermal epithelium of PA2 just below the site of stapes condensation and not in other endoderm epithelia, including the vicinity of malleus-incus condensation (Fig. 6 and Fig. 11B). Interestingly, *Shh*, which is broadly expressed in the

endoderm, is not expressed in the *Bmp4*-expressing region (Fig. 6 and Fig. 11B). The reciprocal expression patterns of *Shh* and *Bmp4* may result from negative regulation between the two pathways, as shown in the endoderm of PA3 where *Bmp4* expression is expanded in *Shh*<sup>-/-</sup> mutants (Moore-Scott and Manley, 2005). *Bmp4* expression in the PA2 endoderm, however, was not changed in *Shh*<sup>-/-</sup> mutants (Moore-Scott and Manley, 2005) or in *Foxg1*<sup>Cre</sup>; *Shh*<sup>lox/lox</sup> mutants, suggesting that SHH exerts differential effects on *Bmp4* expression in different PA positions. The mechanism driving the pattern of *Bmp4* expression in the endoderm at the site of stapes condensation is currently unknown.

Nevertheless, consistent with its definite expression domain, deletion of endodermal *Bmp4* expression (*Foxg1*<sup>Cre</sup>; *Bmp4*<sup>lox/Tm1</sup>) or rendering NCCs unable to mediate BMP signaling (*Wnt1*<sup>Cre</sup>; *Smad4*<sup>lox/lox</sup>) resulted in loss of condensation for the stapes but not for the malleus-incus (Fig. 11E,F). Previous studies using transgenic mice or chicken explant cultures have shown that BMP2/4 signaling plays crucial roles in NCC migration and also directly or indirectly provides positional information to NCCs and induces *Sox9* expression (Kanzler et al., 2000; Kumar et al., 2012; Saito et al., 2012; Semba et al., 2000). *Xnoggin* transgenic mice, in which BMP2/4 signaling is inactivated in the NCCs populating the PA2 and more



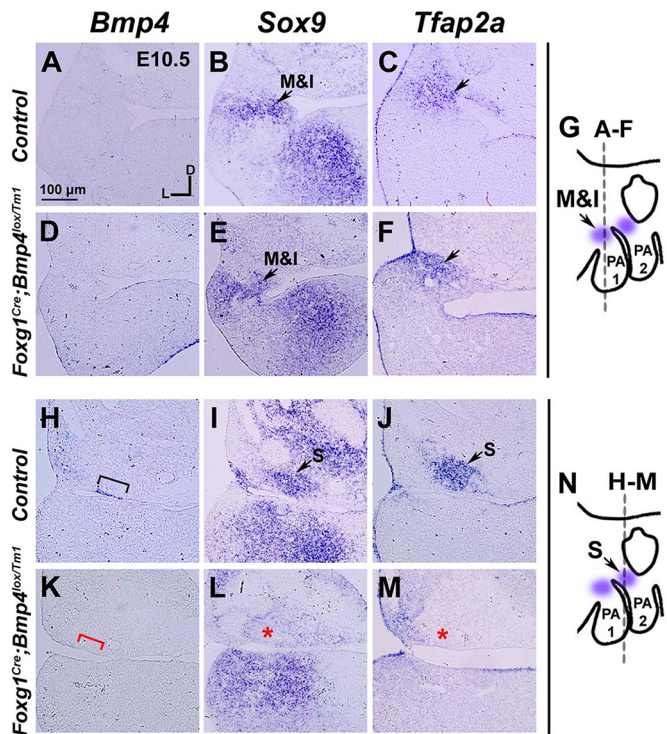


**Fig. 9. Deletion of *Bmp4* in the pharyngeal endoderm results in loss of initial condensation of stapes but not of malleus-incus.** (A-M) Expression of *Bmp4* (A,D,H,K), *Sox9* (B,E,I,L) and *Tfap2a* (C,F,J,M) was compared in the malleus-incus (A-F) and stapes (H-M) regions of control (A-C,H-J) and *Foxg1<sup>Cre</sup>; Bmp4<sup>lox/Tm1</sup>* (D-F,K-M) embryos. The *Bmp4* expression in the pharyngeal endoderm observed in control (H; black bracket) was lost in *Foxg1<sup>Cre</sup>; Bmp4<sup>lox/Tm1</sup>* embryos (K; red bracket). *Sox9* and *Tfap2a* expression in the malleus-incus region was not changed in *Foxg1<sup>Cre</sup>; Bmp4<sup>lox/Tm1</sup>* embryos (B,C,E,F; arrows). In contrast, *Sox9* and *Tfap2a* expression in the stapes regions observed in control (I,J) was lost in *Foxg1<sup>Cre</sup>; Bmp4<sup>lox/Tm1</sup>* embryos (L,M; red asterisks). (G,N) Schematics of E10.5 mouse embryos showing the section planes (indicated by dashed lines) used for malleus-incus (G) and stapes (N) analysis. I, incus; M, malleus; S, stapes. In all images, dorsal is up and lateral is left. Scale bar: 100  $\mu$ m.

caudal PAs, fail to form the skeletal structures derived from the targeted PAs including the stapes (Kanzler et al., 2000). Implantation of BMP4 protein-soaked beads into chicken PA2 mesenchyme or into mouse mandibular explants induced *Sox9* expression, indicating that BMP4 is sufficient to induce mesenchymal condensation (Kumar et al., 2012; Semba et al., 2000). The transplantation of pharyngeal endoderm into chicken embryos altered the morphology of the columella (a structure analogous to middle ear ossicles in mammals) (Zou et al., 2012). Based on these chicken explants results and our mouse studies here, we postulate that endodermal *Bmp4* has a conserved role in middle ear ossicle formation.

#### Endodermal BMP4 signaling directs NCCs to migrate into the prospective stapes region

The lineage-tracing analysis that we performed in *Wnt1-Cre; Smad4<sup>lox/lox</sup>; R26R* mice showed that *lacZ*-positive NCC derivatives were specifically depleted from the prospective stapes condensation area, whereas extensive *lacZ*-positive NCC derivatives populated other mesenchymal areas of PAs (Fig. 7). Thus, the loss of stapes condensation observed in *Wnt1-Cre; Smad4<sup>lox/lox</sup>* embryos appears to result from a failure of NCC migration into the prospective stapes region. Similarly, upon deletion of endodermal *Bmp4* expression, *Tfap2a* expression, which indicates NCC migration,

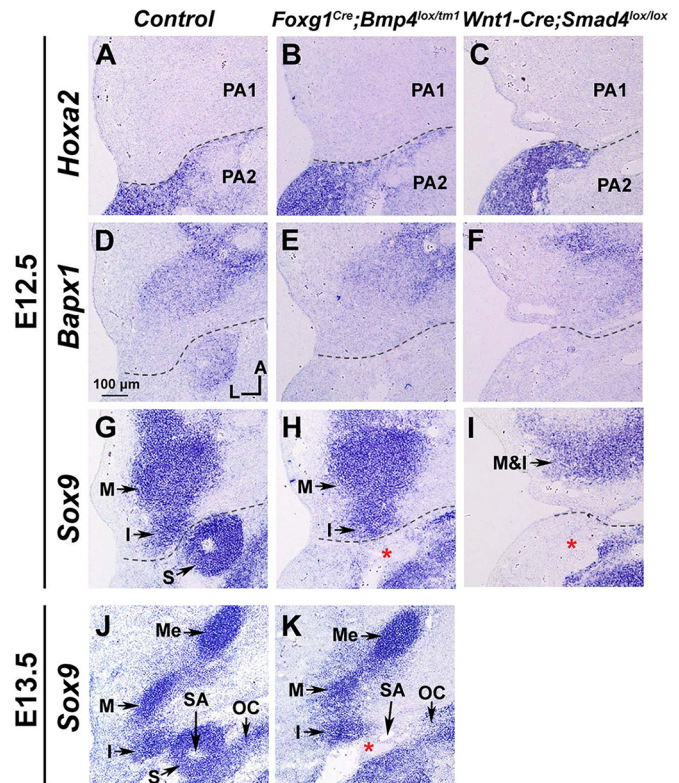


**Fig. 10. Middle ear phenotypes in mutants with loss of TGF $\beta$ /BMP function.** (A-K) Expression patterns of *Hoxa2* (A-C), *Bapx1* (D-F) and *Sox9* (G-K) were compared between control (A,D,G,J), *Foxg1<sup>Cre</sup>; Bmp4<sup>lox/Tm1</sup>* (B,E,H,K) and *Wnt1-Cre; Smad4<sup>lox/lox</sup>* (C,F,I) embryos at E12.5 (A-I) and E13.5 (J,K). *Hoxa2* (A-C) and *Bapx1* (D-F) expression domains indicate the mesenchyme of PA2 and PA1, respectively. Dashed line delineates the border between these domains. *Sox9* expression in the stapes region was specifically abolished in *Foxg1<sup>Cre</sup>; Bmp4<sup>lox/Tm1</sup>* mutant embryos at E12.5 and E13.5 (H,K; red asterisks) and in *Wnt1-Cre; Smad4<sup>lox/lox</sup>* mutant embryos at E12.5 (I; red asterisk). I, incus; M, malleus; Me, Meckel's cartilage; OC, otic capsule; S, stapes; SA, stapedia artery. In all images, anterior is up and lateral is left. Scale bar: 100  $\mu$ m.

was abolished in the prospective stapes condensation area but not in the prospective malleus-incus condensation area (Fig. 9). These results suggest that BMP4 signaling emanating from the endodermal epithelium attracts migratory NCCs to populate the prospective stapes region and to initiate mesenchymal condensation.

How does endodermal BMP4 signaling direct the migrating NCCs to populate the future stapes condensation region? Thus far, several receptor/ligand complexes, such as Eph/ephrin, Nrp/Sema and Cxcl12/Cxcr4, have been implicated in directional NCC migration through roles as chemoattractant or -repellent factors (Minoux and Rijli, 2010). For example, ephrin B1 expressed in the pharyngeal cleft between PA1 and PA2 directs NCCs expressing EphA4 and EphB1/B3 into PA2 (Adams et al., 2001). The interaction between the chemokine CXCL12 and its receptor CXCR4 is of particular interest. *Cxcl12* is expressed in the ectoderm and pharyngeal endoderm at the time of NCC migration into the PAs, whereas *Cxcr4* is expressed in the migrating NCCs (Escot et al., 2016). Defective CXCR4 signaling in both zebrafish and chicken embryos has been shown to result in craniofacial and neural anomalies due to aberrant NCC migration defects (Escot et al., 2016; Olesnick Killian et al., 2009). In addition, CXCL12 acts as a chemoattractant for NCC migration in sympatho-adrenal specification (Saito et al., 2012). Interestingly, BMP signaling

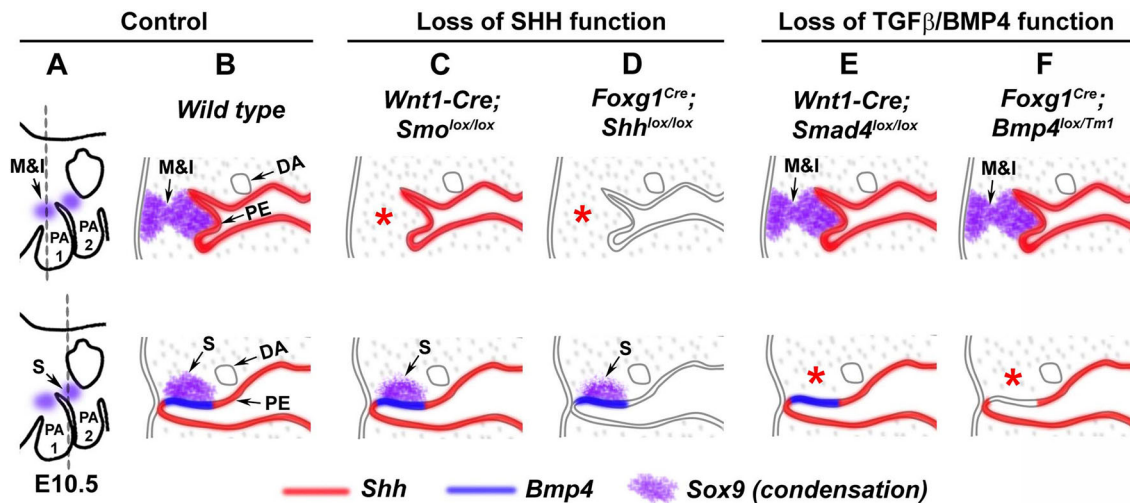


**Fig. 11. Summary of middle ear condensation phenotypes.** (A) Schematics of E10.5 mouse embryos showing the section planes (indicated by dashed lines) depicted in B-F for the initial condensation of malleus-incus (top; M&I) in pharyngeal arch 1 (PA1) and of stapes (bottom; S) in pharyngeal arch 2 (PA2). (B) In wild type, the initial malleus-incus condensation (top row, purple) is located in the mesenchyme lateral to the pharyngeal endoderm, which expresses *Shh* (red line). In contrast, the initial stapes condensation (bottom row, purple) is located in the mesenchyme above the pharyngeal endodermal region where *Bmp4* (blue line) but not *Shh* (red line) is expressed. (C,D) Inactivation of SHH signaling by deleting *Smo* in the NCC derivatives (C; *Wnt1-Cre; Smo<sup>lox/lox</sup>*) or deletion of endodermal *Shh* (D; *Foxg1<sup>Cre</sup>; Smo<sup>lox/lox</sup>*) results in the loss of initial condensation of malleus-incus (red asterisk) but not of stapes. (E,F) Inactivation of TGF $\beta$ /BMP signaling by deleting *Smad4* in the NCC derivatives (E; *Wnt1-Cre; Smad4<sup>lox/lox</sup>*) or deletion of endodermal *Bmp4* (F; *Foxg1<sup>Cre</sup>; Bmp4<sup>lox/Tm1</sup>*) results in the loss of initial condensation of stapes (red asterisk) but not of malleus-incus. DA, dorsal aorta; I, incus; M, malleus; PE, pharyngeal endoderm; S, stapes.

emanating from the dorsal aorta is required for *Cxcl12* expression in the para-aortic mesenchyme (Saito et al., 2012). It will be interesting to determine whether endodermal BMP4 signaling in PA2 dictates NCC migration by promoting expression of *Cxcl12* in the prospective stapes region.

## Conclusions

Our results demonstrate that endodermal SHH signaling is crucial for NCCs to initiate mesenchymal condensation for the malleus and incus in PA1. Based on the lineage and TUNEL analyses, we postulate that in the absence of SHH, NCCs reach the appropriate location in PA1 but fail to thrive and condense to form the malleus and incus. By contrast, BMP4 emanating from the endoderm of PA2 is required for NCCs to initiate stapes formation. Owing to the absence of NCC lineage cells in the prospective stapes region in PA2 and the lack of apparent cell death in the region when NCCs become unresponsive to BMP signaling, we postulate that the lack of BMP4 signaling fails to attract NCCs to the correct location and thereby affects stapes formation. Additionally, although SHH is not required for the mesenchymal condensation of the stapes, it is required for the maintenance of the condensed mesenchyme. Together, these results demonstrate that region-specific interactions between the migratory NCCs and the pharyngeal endoderm play a crucial role in guiding NCCs to migrate to the proper locations and differentiate into specific middle ear ossicles. Further studies aiming to identify other signaling molecules that cooperate with these endodermal signals in the formation of middle ear ossicles will help to elucidate the pathology of ossicular anomalies leading to conductive hearing loss.

## MATERIALS AND METHODS

### Mice

The generation of *Wnt1-Cre; Smo<sup>lox/lox</sup>*, *Wnt1-Cre; SmoM2* (Jeong et al., 2004), *Wnt1-Cre; Smad4<sup>lox/lox</sup>* (Ko et al., 2007), *Foxg1<sup>Cre</sup>; Shh<sup>lox/lox</sup>* (Bok et al., 2013) and *Foxg1<sup>Cre</sup>; Bmp4<sup>lox/Tm1</sup>* (Chang et al., 2008) mice was previously described. A *ROSA26* conditional reporter line (*R26R*) was used

to label NCC derivatives (Soriano, 1999). Littermates carrying genotypes other than the above-mentioned conditional knockouts were used as controls. *Wnt1-Cre; Smad4<sup>lox/lox</sup>; R26R* embryos were generated by mating *Wnt1-Cre; Smad4<sup>lox/+</sup>* mice with *Smad4<sup>lox/lox</sup>; R26R* mice. Similarly, *Wnt1-Cre; Smo<sup>lox/lox</sup>; R26R* embryos were generated by mating *Wnt1-Cre; Smo<sup>lox/+</sup>* mice with *Smo<sup>lox/+</sup>; R26R* mice. All animal protocols were approved by the Institutional Animal Care and Use Committee at Yonsei University College of Medicine.

### In situ hybridization

Antisense RNA probes for *Bmp4* (Morsli et al., 1998), *Sox9* (Wright et al., 1995), *Ptch1* (Goodrich et al., 1996), *Shh* (Echelard et al., 1993), *Acan* (Sandell et al., 1991), *Tfap2a* (+513-+1287, NM\_001122948.2), *Bapx1* (+720-1438, NM\_007524.3) and *Hoxa2* (+671-+1470, NM\_010451.2) were labeled with digoxigenin. *In situ* hybridization was performed as previously described (Morsli et al., 1998). The micrographs of gene expression patterns were acquired using Olympus BX40 and Leica DM2500 optical microscopes. All *in situ* hybridization figures are representative of at least three different samples in two or more independent experiments.

### lacZ detection

Embryos were fixed in 2% paraformaldehyde, 2 mM MgCl<sub>2</sub> and 5 mM EGTA for 2 h at 4°C, dehydrated in 30% sucrose overnight at 4°C, and frozen in OCT compound (Tissue-Tek). Frozen embryos were sectioned at a thickness of 12  $\mu$ m using a cryostat (HM 525, Thermo Scientific) and stained with 5 mM K<sub>3</sub>Fe(CN)<sub>6</sub>, 5 mM K<sub>4</sub>Fe(CN)<sub>6</sub>, 2 mM MgCl<sub>2</sub>, 0.02% NP-40, 1 mg/ml X-gal and 1 $\times$  PBS at 37°C overnight. Micrographs of the X-gal-stained sections were acquired using Olympus BX40 and Leica DM2500 optical microscopes. All *lacZ* detection experiments were performed in at least three different embryos.

### Cell proliferation assay

Cell proliferation was performed using a Click-iT EdU imaging kit (C10337, Thermo Fisher Scientific). Each pregnant mouse was injected three times with 10 mg/kg body weight EdU at 2-h intervals. Two hours after the final injection, embryos were harvested and fixed in 4% paraformaldehyde (PFA) in 1 $\times$  PBS overnight at 4°C. Embryos were then dehydrated in a 30% sucrose solution overnight at 4°C and finally frozen in OCT compound (Tissue-Tek). The embryos were sectioned at a thickness of

12 µm onto Superfrost Plus slides (Tissue-Tek) using a cryostat (HM 525, Thermo Scientific) and then stored at  $-20^{\circ}\text{C}$  until use. The sections were incubated with 500 µl freshly prepared EdU detection solution, which was prepared according to the manufacturer's instructions, for 30 min. This solution contained 430 µl of 1× Click-iT reaction buffer, 20 µl of  $\text{CuSO}_4$ , 1.2 µl Alexa Fluor 488 azide and 50 µl 1× freshly made reaction buffer additive in deionized water (RBA). Nuclear staining with 5 µg/ml Hoechst 33342 was performed for 30 min. After washing with 1× PBS, the slides were mounted with ProLong Gold antifade reagent (Thermo Fisher Scientific). Micrographs of EdU-positive cells were acquired with a Nikon eclipse Ti-U fluorescence microscope.

### Cell death assay

The cell death assay was performed using the ApoptTag Plus Peroxidase In Situ Apoptosis Detection Kit (Millipore, S7101), which detects apoptotic cells by labeling DNA strand breaks by the indirect TUNEL method. Embryos were harvested and fixed in 4% PFA in 1× PBS overnight at  $4^{\circ}\text{C}$ , dehydrated in 30% sucrose solution overnight at  $4^{\circ}\text{C}$ , and finally frozen in OCT compound (Tissue-Tek). The embryos were sectioned at a thickness of 12 µm on Superfrost Plus slides (Tissue-Tek) using a cryostat (HM 525, Thermo Scientific) and were stored at  $-20^{\circ}\text{C}$ . The staining method was performed according to the manufacturer's protocol. In brief, the sections were fixed in 1% PFA in 1× PBS, permeabilized in 2:1 pre-cooled ethanol:acetic acid, incubated in 3%  $\text{H}_2\text{O}_2$ , equilibrated in equilibration buffer, incubated with TdT enzyme in a humidifying chamber for 1 h, and then incubated for 10 min in stop/wash buffer. Then, these sections were conjugated with anti-digoxigenin peroxidase, stained with peroxidase substrate (DAB substrate), and finally counterstained with 1% Methyl Green solution. The slides were then mounted using Permount Mounting Medium (17986, EMS). Micrographs were acquired using a Leica DM2500 optical microscope.

### Cell counting and statistical analysis

Adjacent sections to those used for EdU or TUNEL analysis were used for *in situ* hybridization for *Sox9* to identify the middle ear condensation regions. Cell counting was performed within the rectangular area for malleus-incus condensation (225 µm×90 µm) and stapedial condensation (90 µm×84 µm). The investigators were blind to the genotypes of the controls and conditional knockouts until the completion of cell counting. All cell counts were determined for at least three different embryos for each genotype. Data are displayed as box plots, which were generated using the BoxPlotR web tool (<http://shiny.chemgrid.org/boxplotr/>). Statistical analyses were conducted using Microsoft Excel (Microsoft) and SPSS statistics 23 software (IBM). Two-tailed, unpaired Student's *t*-tests were used to determine statistical significance.  $P < 0.05$  was considered as significant.

### Acknowledgements

We thank Dr Doris K. Wu for critical reading of the manuscript, and Mr Dong Jin Lee, Mr Duyeol Han, and Mr Iljin Bang for their technical assistance. We also thank Dr Brigid Hogan for *Bmp4<sup>lox/lox</sup>* and *Bmp4<sup>Tm1+</sup>* mice and Dr Yu Lan for arranging the shipment of *Smad4<sup>lox/lox</sup>* mice.

### Competing interests

The authors declare no competing or financial interests.

### Author contributions

Conceptualization: H.A., U.-K.K., J.B.; Methodology: H.A., H.M., U.-K.K., J.B.; Validation: H.A., H.M., J.Y.K.; Formal analysis: H.A., H.M., J.Y.K.; Investigation: H.A., H.M., J.Y.K.; Resources: X.Y., E.-S.C.; Writing - original draft: H.A., U.-K.K., J.B.; Writing - review & editing: H.A., U.-K.K., J.B.; Visualization: H.A., U.-K.K., J.B.; Supervision: J.B.; Project administration: J.B.; Funding acquisition: U.-K.K., J.B.

### Funding

This work was supported by grants from the National Research Foundation of Korea (NRF-2014M3A9D5A01073865 to U.-K.K. and J.B.; NRF-2016R1A5A2008630 and NRF-2017R1A2B3009133 to J.B.).

### Supplementary information

Supplementary information available online at <http://dev.biologists.org/lookup/doi/10.1242/dev.167965.supplemental>

### References

- Abu-Issa, R., Smyth, G., Smoak, I., Yamamura, K. and Meyers, E. N. (2002). Fgf8 is required for pharyngeal arch and cardiovascular development in the mouse. *Development* **129**, 4613-4625.
- Adams, R. H., Diella, F., Hennig, S., Helmbacher, F., Deutsch, U. and Klein, R. (2001). The cytoplasmic domain of the ligand ephrinB2 is required for vascular morphogenesis but not cranial neural crest migration. *Cell* **104**, 57-69.
- Ahlgren, S. C. and Bronner-Fraser, M. (1999). Inhibition of sonic hedgehog signaling in vivo results in craniofacial neural crest cell death. *Curr. Biol.* **9**, 1304-1314.
- Anthwal, N. and Thompson, H. (2016). The development of the mammalian outer and middle ear. *J. Anat.* **228**, 217-232.
- Bandyopadhyay, A., Tsuji, K., Cox, K., Harfe, B. D., Rosen, V. and Tabin, C. J. (2006). Genetic analysis of the roles of BMP2, BMP4, and BMP7 in limb patterning and skeletogenesis. *PLoS Genet.* **2**, e216.
- Bhatt, S., Diaz, R. and Trainor, P. A. (2013). Signals and switches in Mammalian neural crest cell differentiation. *Cold Spring Harb. Perspect Biol.* **5**, a008326.
- Billmyre, K. K. and Klingensmith, J. (2015). Sonic hedgehog from pharyngeal arch 1 epithelium is necessary for early mandibular arch cell survival and later cartilage condensation differentiation. *Dev. Dyn.* **244**, 564-576.
- Bok, J., Zenczak, C., Hwang, C. H. and Wu, D. K. (2013). Auditory ganglion source of Sonic hedgehog regulates timing of cell cycle exit and differentiation of mammalian cochlear hair cells. *Proc. Natl. Acad. Sci. USA* **110**, 13869-13874.
- Brito, J. M., Teillet, M.-A. and Le Douarin, N. M. (2006). An early role for sonic hedgehog from foregut endoderm in jaw development: ensuring neural crest cell survival. *Proc. Natl. Acad. Sci. USA* **103**, 11607-11612.
- Chai, Y., Jiang, X., Ito, Y., Bringas, P., Jr., Han, J., Rowitch, D. H., Soriano, P., McMahon, A. P. and Sucov, H. M. (2000). Fate of the mammalian cranial neural crest during tooth and mandibular morphogenesis. *Development* **127**, 1671-1679.
- Chang, W., Lin, Z., Kulesa, H., Hébert, J., Hogan, B. L. M. and Wu, D. K. (2008). Bmp4 is essential for the formation of the vestibular apparatus that detects angular head movements. *PLoS Genet.* **4**, e1000050.
- Chapman, S. C. (2011). Can you hear me now? Understanding vertebrate middle ear development. *Front. Biosci.* **16**, 1675-1692.
- Couly, G., Creuzet, S., Bennaceur, S., Vincent, C. and Le Douarin, N. M. (2002). Interactions between Hox-negative cephalic neural crest cells and the foregut endoderm in patterning the facial skeleton in the vertebrate head. *Development* **129**, 1061-1073.
- Echelard, Y., Epstein, D. J., St-Jacques, B., Shen, L., Mohler, J., McMahon, J. A. and McMahon, A. P. (1993). Sonic hedgehog, a member of a family of putative signaling molecules, is implicated in the regulation of CNS polarity. *Cell* **75**, 1417-1430.
- Escot, S., Blavet, C., Faure, E., Zaffran, S., Duband, J.-L. and Fournier-Thibault, C. (2016). Disruption of CXCR4 signaling in pharyngeal neural crest cells causes DiGeorge syndrome-like malformations. *Development* **143**, 582-588.
- Goodrich, L. V., Johnson, R. L., Milenkovic, L., McMahon, J. A. and Scott, M. P. (1996). Conservation of the hedgehog/patched signaling pathway from flies to mice: induction of a mouse patched gene by Hedgehog. *Genes Dev.* **10**, 301-312.
- Hébert, J. M. and McConnell, S. K. (2000). Targeting of cre to the Foxg1 (BF-1) locus mediates loxP recombination in the telencephalon and other developing head structures. *Dev. Biol.* **222**, 296-306.
- Jeong, J., Mao, J., Tenzen, T., Kottmann, A. H. and McMahon, A. P. (2004). Hedgehog signaling in the neural crest cells regulates the patterning and growth of facial primordia. *Genes Dev.* **18**, 937-951.
- Kanzler, B., Foreman, R. K., Labosky, P. A. and Mallo, M. (2000). BMP signaling is essential for development of skeletogenic and neurogenic cranial neural crest. *Development* **127**, 1095-1104.
- Ko, S. O., Chung, I. H., Xu, X., Oka, S., Zhao, H., Cho, E. S., Deng, C. and Chai, Y. (2007). Smad4 is required to regulate the fate of cranial neural crest cells. *Dev. Biol.* **312**, 435-447.
- Kumar, M., Ray, P. and Chapman, S. C. (2012). Fibroblast growth factor and bone morphogenetic protein signaling are required for specifying prechondrogenic identity in neural crest-derived mesenchyme and initiating the chondrogenic program. *Dev. Dyn.* **241**, 1091-1103.
- Minoux, M. and Rijli, F. M. (2010). Molecular mechanisms of cranial neural crest cell migration and patterning in craniofacial development. *Development* **137**, 2605-2621.
- Moore-Scott, B. A. and Manley, N. R. (2005). Differential expression of Sonic hedgehog along the anterior-posterior axis regulates patterning of pharyngeal pouch endoderm and pharyngeal endoderm-derived organs. *Dev. Biol.* **278**, 323-335.
- Morsli, H., Choo, D., Ryan, A., Johnson, R. and Wu, D. K. (1998). Development of the mouse inner ear and origin of its sensory organs. *J. Neurosci.* **18**, 3327-3335.
- Olesnicki Killian, E. C., Birkholz, D. A. and Artinger, K. B. (2009). A role for chemokine signaling in neural crest cell migration and craniofacial development. *Dev. Biol.* **333**, 161-172.
- Ozeki-Satoh, M., Ishikawa, A., Yamada, S., Uwabe, C. and Takakuwa, T. (2016). Morphogenesis of the middle ear ossicles and spatial relationships with the external and inner ears during the embryonic period. *Anat. Rec.* **299**, 1325-1337.

- Quesnel, S., Benchaa, T., Bernard, S., Martine, F., Viala, P., Van Den Abbeele, T. and Teissier, N.** (2015). Congenital middle ear anomalies: anatomical and functional results of surgery. *Audiol. Neurootol.* **20**, 237-242.
- Saito, D., Takase, Y., Murai, H. and Takahashi, Y.** (2012). The dorsal aorta initiates a molecular cascade that instructs sympatho-adrenal specification. *Science* **336**, 1578-1581.
- Sandell, L. J., Morris, N., Robbins, J. R. and Goldring, M. B.** (1991). Alternatively spliced type II procollagen mRNAs define distinct populations of cells during vertebral development: differential expression of the amino-propeptide. *J. Cell Biol.* **114**, 1307-1319.
- Semba, I., Nonaka, K., Takahashi, I., Takahashi, K., Dashner, R., Shum, L., Nuckolls, G. H. and Slavkin, H. C.** (2000). Positionally-dependent chondrogenesis induced by BMP4 is co-regulated by Sox9 and Msx2. *Dev. Dyn.* **217**, 401-414.
- Soriano, P.** (1999). Generalized lacZ expression with the ROSA26 Cre reporter strain. *Nat. Genet.* **21**, 70-71.
- Tavares, A. L. P., Garcia, E. L., Kuhn, K., Woods, C. M., Williams, T. and Clouthier, D. E.** (2012). Ectodermal-derived Endothelin1 is required for patterning the distal and intermediate domains of the mouse mandibular arch. *Dev. Biol.* **371**, 47-56.
- Tavella, S., Biticchi, R., Schito, A., Minina, E., Di Martino, D., Pagano, A., Vortkamp, A., Horton, W. A., Cancedda, R. and Garofalo, S.** (2004). Targeted expression of SHH affects chondrocyte differentiation, growth plate organization, and Sox9 expression. *J. Bone Miner. Res.* **19**, 1678-1688.
- Tavella, S., Biticchi, R., Morello, R., Castagnola, P., Musante, V., Costa, D., Cancedda, R. and Garofalo, S.** (2006). Forced chondrocyte expression of sonic hedgehog impairs joint formation affecting proliferation and apoptosis. *Matrix Biol.* **25**, 389-397.
- Trumpp, A., Depew, M. J., Rubenstein, J. L. R., Bishop, J. M. and Martin, G. R.** (1999). Cre-mediated gene inactivation demonstrates that FGF8 is required for cell survival and patterning of the first branchial arch. *Genes Dev.* **13**, 3136-3148.
- Tucker, A. S., Watson, R. P., Lettice, L. A., Yamada, G. and Hill, R. E.** (2004). Bapx1 regulates patterning in the middle ear: altered regulatory role in the transition from the proximal jaw during vertebrate evolution. *Development* **131**, 1235-1245.
- Wright, E., Hargrave, M. R., Christiansen, J., Cooper, L., Kun, J., Evans, T., Gangadharan, U., Greenfield, A. and Koopman, P.** (1995). The Sry-related gene Sox9 is expressed during chondrogenesis in mouse embryos. *Nat. Genet.* **9**, 15-20.
- Zou, Y., Mak, S.-S., Liu, H. Z., Han, D. Y., Zhuang, H. X., Yang, S. M. and Ladhur, R. K.** (2012). Induction of the chick columella and its integration with the inner ear. *Dev. Dyn.* **241**, 1104-1110.